Electronic Supplementary Material (ESI) for Journal of Materials Chemistry A.


Supplementary Information for

# Interdiffused Thermoplastic Urethane−PEDOT:PSS Bilayers with Superior Adhesion Properties for High−Performance and Intrinsically−Stretchable Organic Solar Cells

*Jinho Lee,*[†,a] *Jin-Woo Lee,*[†,a] *Hyunggwi Song,*[b] *Myoung Song,*[b] *Jinseok Park,* [a] *Geon-U Kim,*[a] *Dahyun Jeong,*[a] *Taek-Soo Kim,*[b] *and Bumjoon J. Kim*[*,a]

[a] Department of Chemical and Biomolecular Engineering and [b] Mechancial Engineering, Korea Advanced Institute of Science and Technology (KAIST), Daejeon 34141, Republic of Korea

*Electronic mail: bumjoonkim@kaist.ac.kr

## Experimental Section

### Materials

PEDOT:PSS (Clevios PH1000 and Clevios P VP AI 4083) solutions were purchased from Heraeus. Perchloric acid ($HClO_4$), chlorobenzene (CB), chloroform (CF), methanol, octadecyltrichlorosilane (ODTS), toluene, 3-glycidoxypropyltrimethoxysilane (GOPS), dimethylformamide (DMF), 1-chloronaphthalene (CN), 1,8-diiodoctane (DIO) and dimethyl Sulfoxide (DMSO) were purchased from Sigma-Aldrich. PM6, PCE12, Y6 and Y6-BO were purchased from Derthon. N2200 polymer (Mn: 150 k, PDI: 3.0) and PNDIT-F3N-Br were synthesized. TPU film was received form AFEL. Gallium (Ga, 99.99 % purity) and Indium (In, 99.99 % purity) were obtained from Taewon Scientific.

### Preparation of acid-treated electrodes for transfer

ODTS hydrophobic treatment was applied to the glass substrate to facilitate the transfer process. After immersing the plasma-treated glass substrate in a mixture of 50 ml of toluene and 60 $\mu$l of ODTS at room temperature for 30 min, it was washed with acetone and dried in an oven at 80 °C. The PEDOT:PSS (doped with 0.5 vol.% of FS-30, 5 vol.% of DMSO and 0.15 vol.% of GOPS) solution was filtered through a 0.45 $\mu$m polytetrafluorethylene (PTFE) filter, and then deposited on the ODTS treated glass substrate by spin-coating (1000 rpm) and dried at 100 °C in air (thickness: ~150 nm). 4 M $HClO_4$ solution was dropwise to the surface of the PEDOT:PSS film, and immediately washed with a spin-dry process, and dried on a hot plate at 100 °C for 15 min to remove residual acid (thickness: ~113 nm). For the molecular interdiffusion (MID)-assisted poly(3,4-ethylenedioxythiophene):poly(styrenesulfonate)-thermoplastic urethane (PEDOT:PSS-TPU) layers, the TPU solution (dissolved in DMF at 450 mg $mL^{-1}$) was spin-coated (4000 rpm) on acid-treated PEDOT:PSS and dried at 100 °C. In the

stamp transfer (ST) method, the pick-and-placed PEDOT:PSS bottom electrode layer was laid to the TPU film while slowly attaching/detaching the TPU film on an 80 °C hot plate.

**Device Fabrication**

IS-OSCs were fabricated with TPU/acid-treated PEDOT:PSS/AI 4083/active layer/PNDIT-F3N-Br/eutectic gallium indium (EGaIn) structure. The transferred TPU/acid-treated PEDOT:PSS electrode was attached to a glass substrate for use as a bottom electrode. The hole transport layer (HTL, Clevios P VP AI 4083, doped with 0.5 vol.% of FS-30) was spin-coated at 3000 rpm (thickness: ~30 nm) on the plasma-treated bottom electrode and then annealed at 100 °C for 15 min. The active material was coated in a glove box. A blend of PM6:Y6-BO:N2200 with a weight ratio (1:1:0.15) was stirred for at least 3 h in CB at a total concentration of 24 mg $mL^{-1}$ and then spin-coated at 2500 rpm, 30 s (thickness: ~100 nm) on top of the TPU/acid-treated PEDOT:PSS/AI4083. A blend of PM6:Y6 (1:1.2, w/w) in CF (containing 0.5 vol% of 1-chloronaphthalene (CN)) with a total concentration of 13.5 mg $mL^{-1}$ solution was spuncast at 2500 rpm for 30 s (thickness: ~100 nm). A blend of PM6-OEG5:BTP-eC9 (1:1.2, w/w) in toluene (containing 0.5 vol% of DIO) with a total concentration of 18 mg $mL^{-1}$ solution was spuncast at 1500 rpm for 30 s (thickness: ~ 110 nm). A blend of PBDB-T:PYBDT-Cl (1:1, w/w) in CB with a total concentration of 20 mg $mL^{-1}$ solution was spun at 2000 rpm for 30 s (thickness: ~100 nm). All devices coated with the active layer were vacuum (< $10^{-5}$ torr) dried for 1 h. Then, an electron transport layer (ETL, PNDIT-F3N-Br) solution (total concentration of 1 mg $mL^{-1}$ in methanol, stirred at room temperature for 3 h) was spin-coated at 3000 rpm for 30 s (thickness: ~5 nm) on the active layer. A top electrode, EGaIn, 75.5 wt% of Ga and 24.5 wt% of In were mixed at 80 °C. To pattern the electrodes, a liquid metal alloy was sprayed (thickness: ~100 $\mu$m) onto the ETL layer using a

shadow mask.

**Characterizations**

The transmission spectrum of the PEDOT:PSS electrode was measured with a UV-vis spectrophotometer (UV-1800, Shimadzu). Sheet resistances of the PEDOT:PSS films were measured by using a four point probe. The ultraviolet photoelectron spectroscopy (UPS) profiles were obtained by Sigma Probe from Thermo VG Scientific Thermo VG Scientific incorporation. The 90 ° peel tests were performed using an adhesion tester (DTS company, 50 lbf load cell) operated at a peeling rate of 0.1 mm $s^{-1}$ with an adhesive tape (12 mm width). The time-of-flight secondary ion mass spectrometry (TOF-SIMS) depth profiling analysis (sputtered with 5 keV $Ar^+$ and 500 × 500 $\mu m^2$) was performed to investigate the interfacial properties between the PEDOT:PSS electrode and the TPU. Relative resistance ($R/R_0$) and tensile cycle test of PEDOT:PSS film were measured using a stretching tester (JIRBT-620, Junil Tech., South Korea). Atomic force microscopy (AFM, Parks Systems NX20) was used to analyze the surface morphology of PEDOT:PSS film. To measure the thickness of PEDOT:PSS film, we used a surface profiler (Tencor α-Step IQ). The PCE was determined under ambient conditions with a solar simulator (K201 LAB55, McScience). The photovoltaic performance was measured under air mass 1.5 solar illumination at 100 mW $cm^{-2}$ (1 sun). The intensity of the solar simulator was calibrated using a standard silicon reference cell (K801S-K302, McScience). The current density-voltage (*J–V*) characteristics were recorded using a Keithley 2400 SMU semiconductor characterization system. A shadow mask (0.04 $cm^2$) was used to define the photoactive area during the measurements. And, we measured the change in properties of IS-OSCs according to elongational deformation using a manually adjustable tensile strain test holder. External quantum efficiency (EQE) spectra were measured by K3100

15 IQX (McScience Inc.) and MC 2000 optical chopper (Thorlabs) under ambient conditions.

**Calculation of FoM value**

The FoM is defined as the ratio of direct current conductivity ($\sigma_{dc}$) to optical conductivity ($\sigma_{op}$). It can be calculated as sheet resistance ($\Omega$ $sq^{-1}$), transmittance (%, at $\lambda$ = 550 nm) and impedance of free space ($Z_0$, 377 $\Omega$).

$$FoM = \frac{\sigma_{dc}}{\sigma_{op}} = \frac{Z_0}{2R_{sheet}\left(T^{-\frac{1}{2}} - 1\right)}$$

**Finite Element Method Simulation**

The relationship between the stretchability and the interfacial adhesion was investigated using a commercial finite element method tool (ABAQUS v 6.24). The TPU-PEDOT:PSS bilayer was modeled as a deformable 3D solid with 226,929 nodes and 210,160 elements of type CSD8R (8-node linear brick, reduced integration, hourglass control). The TPU was considered as a hyperelastic material based on the Arruda-Boyce model (E: 10 MPa, v: 0.45), while the PEDOT:PSS was considered to be elastic material (E: 500 MPa, v: 0.35). To simulate the stretching and cracking process, the boundary conditions of the model were defined as follows: The model was uniaxially tensile loaded with displacement control, and the interfacial adhesion was characterized with a fracture criterion of VCCT. And, planar crack driving force was calculated for a 10 μm long initial crack with the J-integral method.

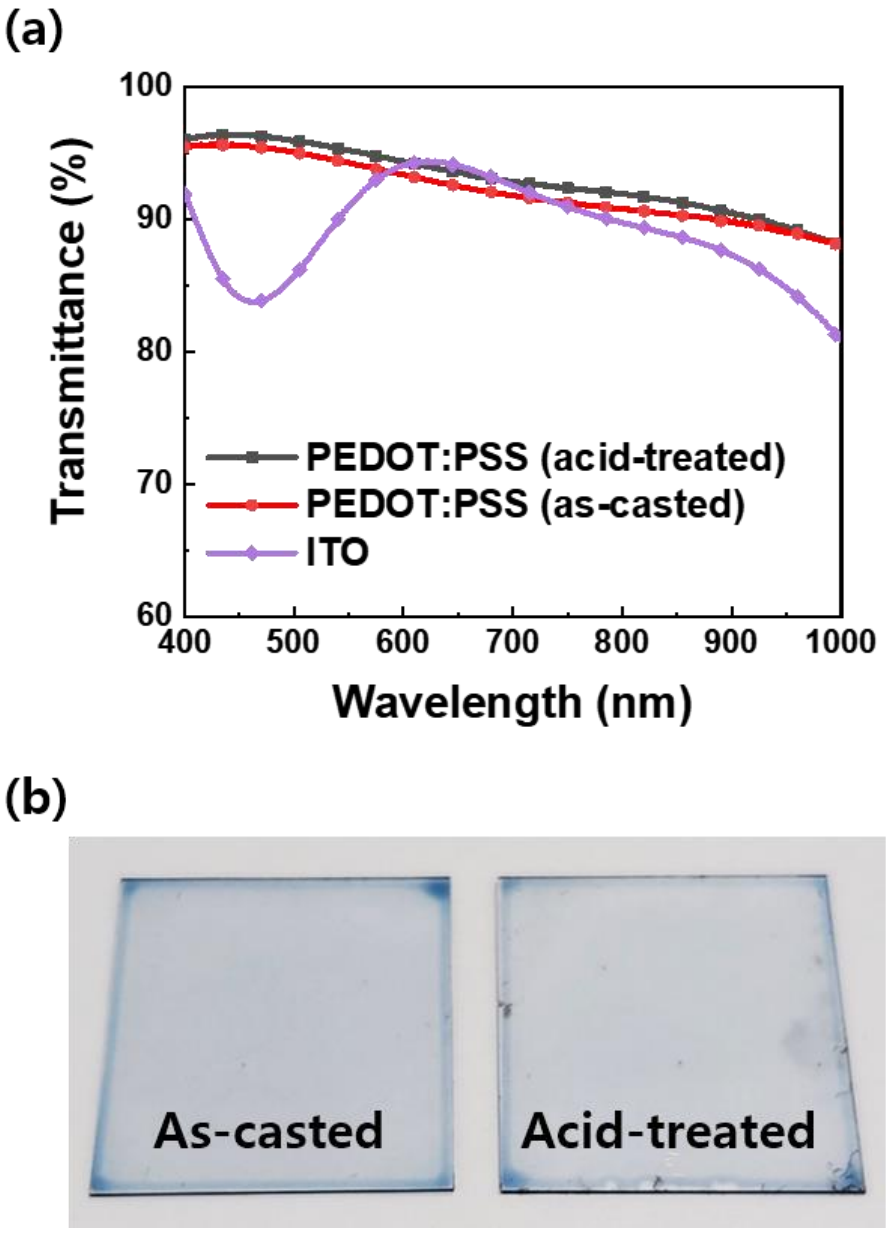


**Fig. S1.** (a) Optical transmittances of as-casted and acid-treated PEDOT:PSS STEs compare with ITO; (b) images of as-casted and acid-treated PEDOT:PSS on ODTS treated glass.

**Table S1.** Sheet resistance, conductivity and work function of PEDOT:PSS depending on acid treatment and transfer method.

| | Substrate | sheet resistance ($\Omega$ sq$^{-1}$) | conductivity (S cm$^{-1}$) | work function (eV) |
|---|---|---|---|---|
| **PEDOT:PSS as-casted** | glass | 110 | 605 | 5.0 |
| **PEDOT:PSS acid-treated** | glass | 92 | 961 | 5.0 |
| | TPU (MID) | 88 | 959 | 5.0 |
| | TPU (ST) | 90 | 958 | 5.0 |

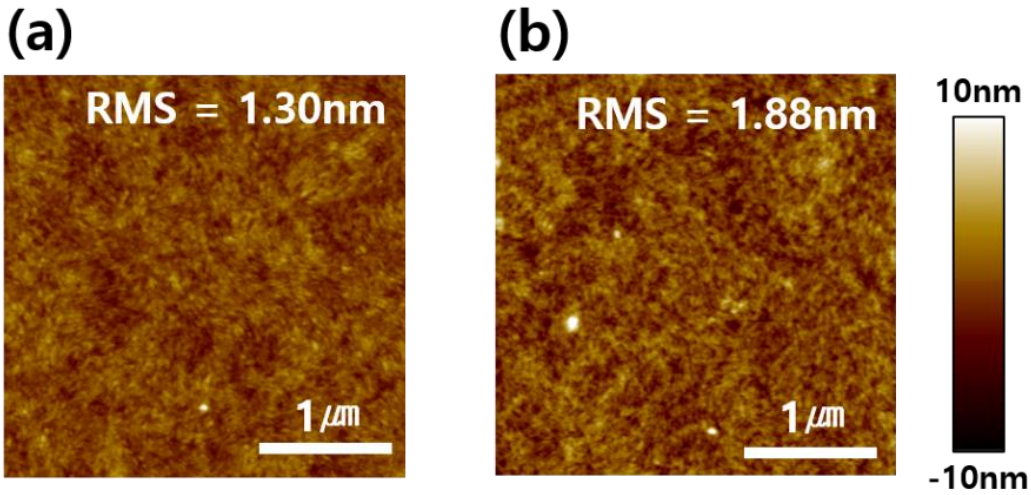


**Fig. S2.** AFM images of (a) as-casted PEDOT:PSS and (b) acid-treated PEDOT:PSS.

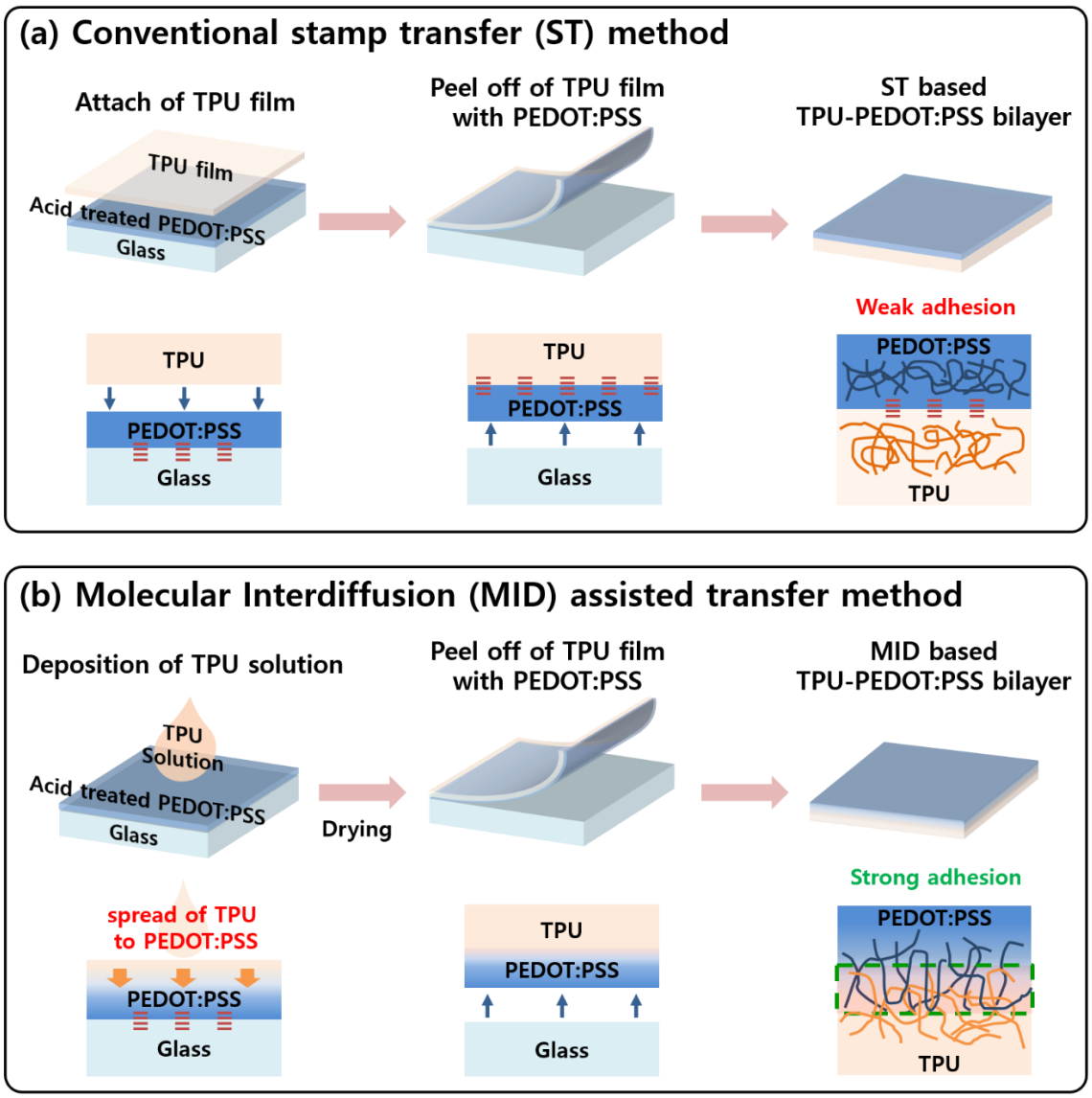


**Fig. S3.** Schematics depicting fabrication procedures of (a) ST- and (b) MID-based TPU-PEDOT:PSS bilayers.

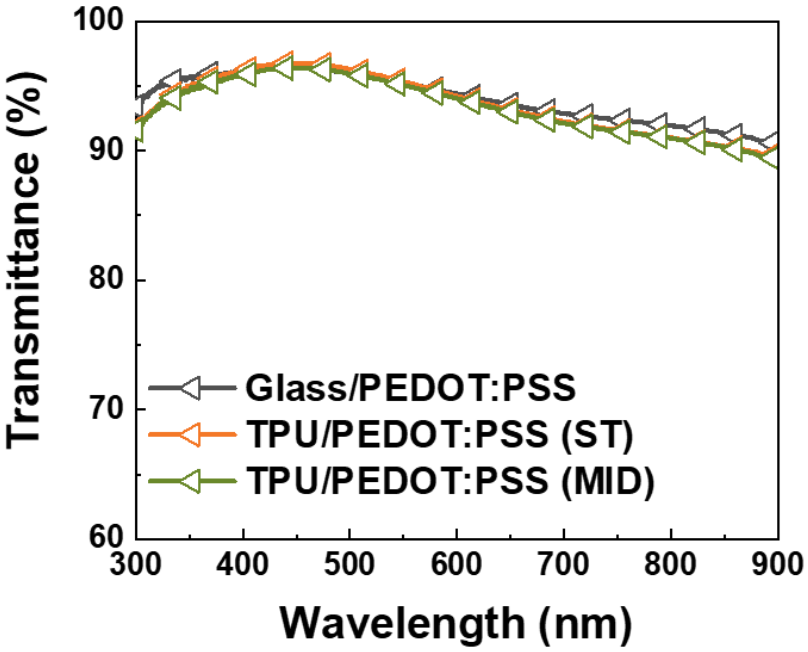


**Fig. S4.** Optical transmittance of PEDOT:PSS STEs on bare glass and on TPU films (ST and MID-assisted).

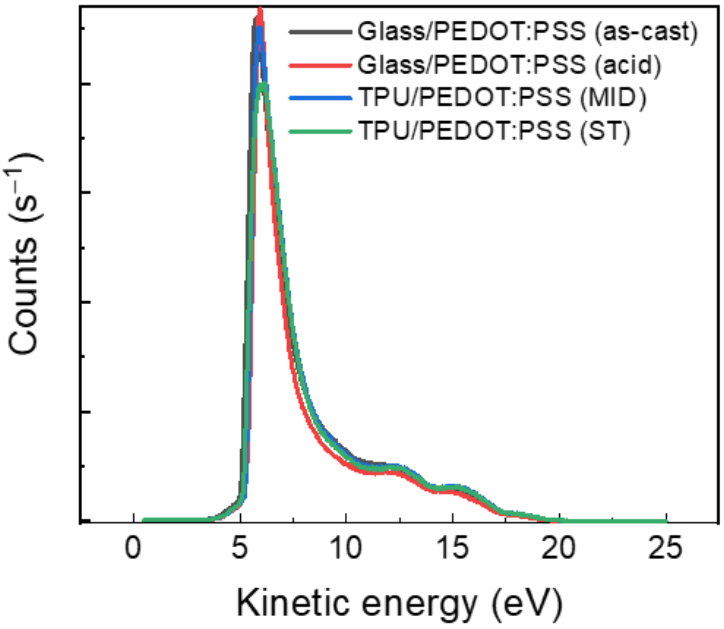


**Fig. S5.** UPS(Ultraviolet photoelectron spectroscopy) profiles of PEDOT:PSS depending on acid treatment and transfer method.

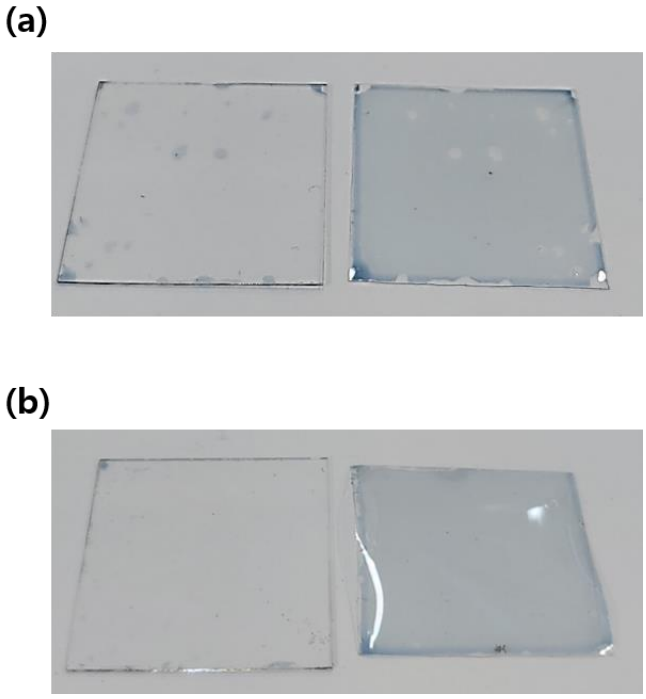


**Fig. S6.** The photographs of (a) ST- and (b) MID-assisted TPU−PEDOT:PSS bilayers (right) from glass substrates (left).

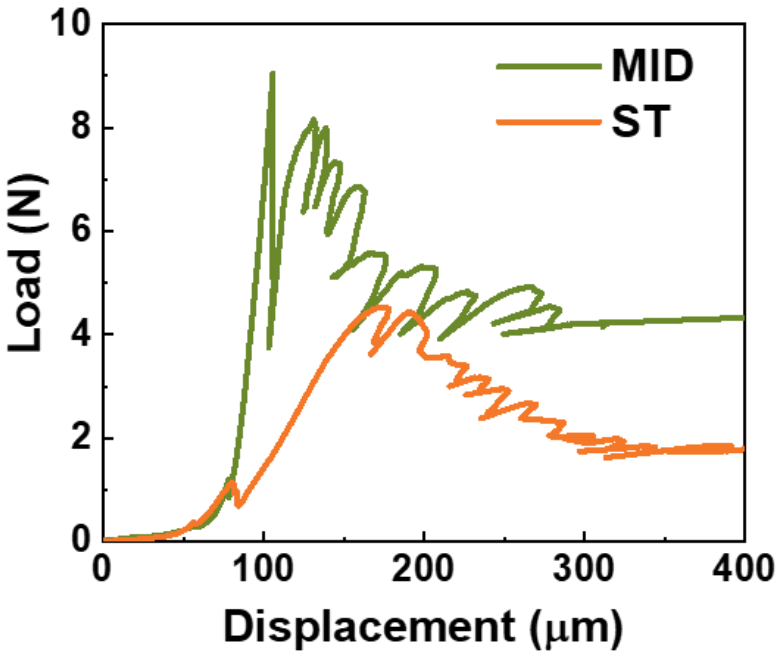


**Fig. S7.** Displacement vs. load profiles of ST- and MID-based TPU-PEDOT:PSS bilayers measured by DCB test.

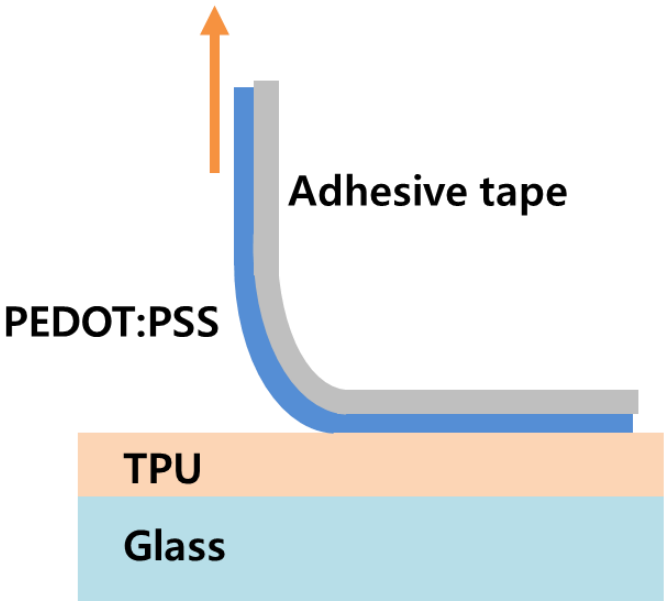


**Fig. S8.** Schematic diagram for the 90° peel test.

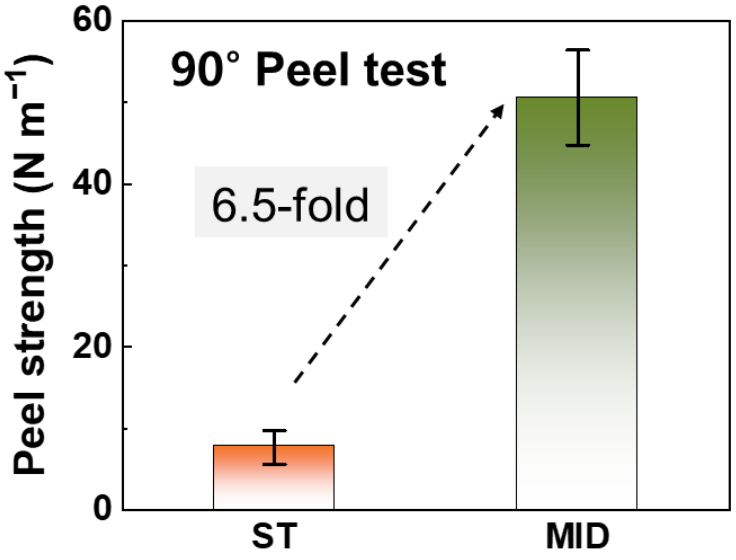


**Fig. S9.** Peel strength of ST- and MID-based bilayers measured from 90° peel test.

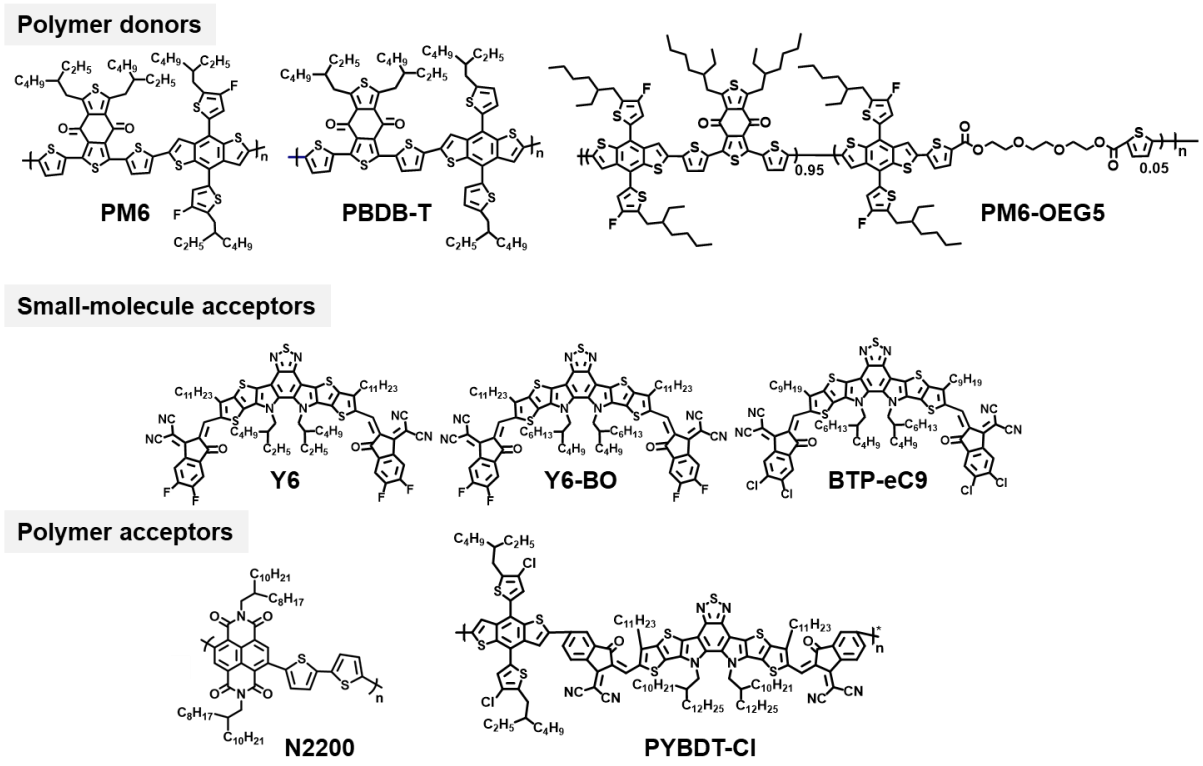


**Fig. S10.** Chemical structures of the active materials used in this study.

**Table S3.** Photovoltaic parameters of the PM6:Y6-BO:N2200-based IS-OSCs with MID-based TPU-PEDOT:PSS as a function of strain.

| **Strain (%)** | $V_{oc}$ **(V)** | $J_{sc}$ **(mA cm$^{-2}$)** | **FF (%)** | **PCE (%)** |
|---|---|---|---|---|
| 0 | 0.85 | 23.2 | 65.9 | 13.1 |
| 10 | 0.86 | 23.1 | 67.4 | 13.4 |
| 20 | 0.86 | 23.3 | 66.9 | 13.5 |
| 30 | 0.86 | 23.8 | 61.7 | 13.0 |
| 40 | 0.85 | 22.3 | 55.3 | 9.4 |
| 50 | 0.85 | 19.7 | 44.3 | 7.5 |

**Table S4.** Photovoltaic parameters of the PM6:Y6-BO:N2200-based IS-OSCs with ST-based TPU-PEDOT:PSS as a function of strain.

| **Strain (%)** | $V_{oc}$ **(V)** | $J_{sc}$ **(mA cm$^{-2}$)** | **FF (%)** | **PCE (%)** |
|---|---|---|---|---|
| 0 | 0.85 | 23.0 | 67.8 | 13.3 |
| 10 | 0.87 | 22.9 | 64.6 | 12.7 |
| 20 | 0.88 | 22.5 | 59.3 | 11.7 |
| 30 | 0.87 | 21.8 | 45.3 | 8.6 |
| 40 | 0.87 | 19.9 | 36.7 | 6.4 |
| 50 | 0.86 | 14.7 | 31.6 | 4.0 |

**Table S5.** Photovoltaic parameters of the PM6:Y6-based IS-OSCs with MID-based TPU-PEDOT:PSS as a function of strain.

| Strain (%) | $V_{oc}$ (V) | $J_{sc}$ (mA cm$^{-2}$) | FF (%) | PCE (%) |
|---|---|---|---|---|
| 0 | 0.81 | 20.44 | 63.54 | 10.56 |
| 10 | 0.82 | 20.50 | 63.00 | 10.65 |
| 20 | 0.82 | 20.33 | 63.53 | 10.61 |
| 30 | 0.83 | 19.62 | 48.48 | 7.86 |
| 40 | 0.80 | 7.92 | 35.18 | 2.22 |
| 50 | 0.78 | 4.05 | 35.52 | 1.12 |

**Table S6.** Photovoltaic parameters of the PM6:Y6-based IS-OSCs with ST-based TPU-PEDOT:PSS as a function of strain.

| Strain (%) | $V_{oc}$ (V) | $J_{sc}$ (mA cm$^{-2}$) | FF (%) | PCE (%) |
|---|---|---|---|---|
| 0 | 0.85 | 20.38 | 60.40 | 10.52 |
| 10 | 0.85 | 20.35 | 59.16 | 10.24 |
| 20 | 0.85 | 20.09 | 51.25 | 8.75 |
| 30 | 0.53 | 13.21 | 31.87 | 2.23 |
| 40 | 0.51 | 12.95 | 29.53 | 1.95 |
| 50 | 0.41 | 10.68 | 24.22 | 1.06 |

**Table S7.** Photovoltaic parameters of the PM6-OEG5:BTP-eC9-based IS-OSCs with MID-based TPU-PEDOT:PSS as a function of strain.

| Strain (%) | $V_{oc}$ (V) | $J_{sc}$ (mA cm$^{-2}$) | FF (%) | PCE (%) |
|---|---|---|---|---|
| 0 | 0.86 | 23.43 | 63.08 | 12.69 |
| 10 | 0.86 | 23.69 | 63.96 | 13.03 |
| 20 | 0.86 | 23.99 | 61.70 | 12.74 |
| 30 | 0.85 | 20.57 | 57.45 | 10.02 |
| 40 | 0.84 | 22.59 | 49.21 | 9.31 |
| 50 | 0.82 | 19.52 | 43.41 | 6.98 |

**Table S8.** Photovoltaic parameters of the PM6-OEG5:BTP-eC9-based IS-OSCs with ST-based TPU-PEDOT:PSS as a function of strain.

| Strain (%) | $V_{oc}$ (V) | $J_{sc}$ (mA cm$^{-2}$) | FF (%) | PCE (%) |
|---|---|---|---|---|
| 0 | 0.85 | 23.48 | 62.10 | 12.38 |
| 10 | 0.84 | 23.25 | 62.10 | 12.11 |
| 20 | 0.85 | 22.52 | 58.37 | 11.11 |
| 30 | 0.82 | 14.56 | 37.81 | 4.52 |
| 40 | 0.83 | 10.57 | 25.46 | 2.24 |
| 50 | 0.82 | 9.16 | 19.87 | 1.49 |

**Table S9.** Photovoltaic parameters of the PBDB-T:PYBDT-Cl-based IS-OSCs with MID-based TPU-PEDOT:PSS as a function of strain.

| Strain (%) | $V_{oc}$ (V) | $J_{sc}$ (mA cm$^{-2}$) | FF (%) | PCE (%) |
|---|---|---|---|---|
| 0 | 0.89 | 17.77 | 67.74 | 10.77 |
| 10 | 0.89 | 18.00 | 65.54 | 10.52 |
| 20 | 0.90 | 16.51 | 70.30 | 10.44 |
| 30 | 0.88 | 15.41 | 61.14 | 8.26 |
| 40 | 0.88 | 15.91 | 58.08 | 8.09 |
| 50 | 0.84 | 15.63 | 50.84 | 6.70 |

**Table S10.** Photovoltaic parameters of the PBDB-T:PYBDT-Cl-based IS-OSCs with ST-based TPU-PEDOT:PSS as a function of strain.

| Strain (%) | $V_{oc}$ (V) | $J_{sc}$ (mA cm$^{-2}$) | FF (%) | PCE (%) |
|---|---|---|---|---|
| 0 | 0.90 | 18.39 | 69.93 | 11.53 |
| 10 | 0.90 | 17.04 | 70.95 | 10.85 |
| 20 | 0.88 | 15.26 | 58.28 | 7.86 |
| 30 | 0.69 | 14.47 | 38.94 | 3.88 |
| 40 | 0.45 | 11.78 | 34.05 | 1.79 |
| 50 | 0.42 | 9.77 | 32.74 | 1.34 |

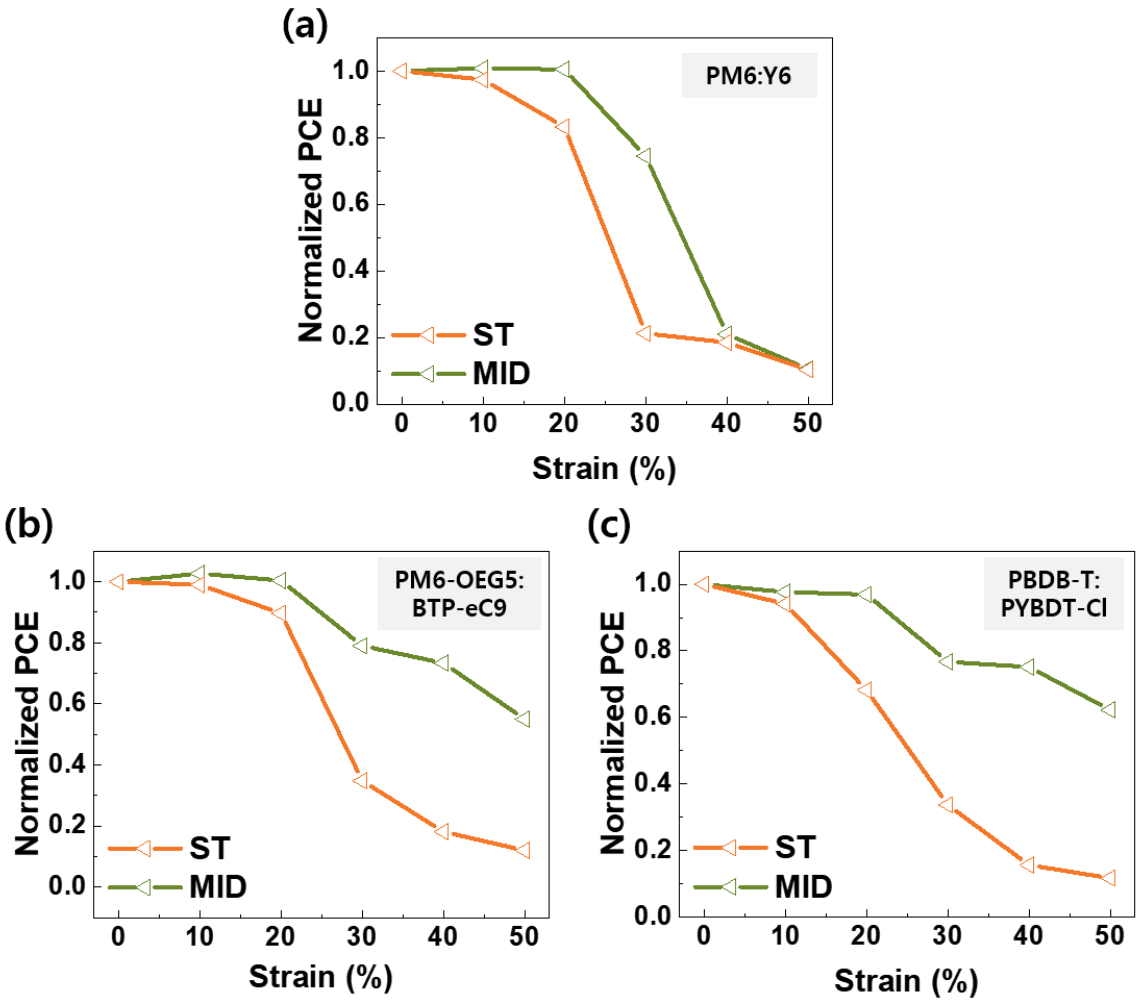


**Fig. S11.** PCE of (a) PM6:Y6, (b) PM6-OEG5:BTP-eC9 and (c) PBDB-T:PYBDT-Cl based IS-OSCs under strains.

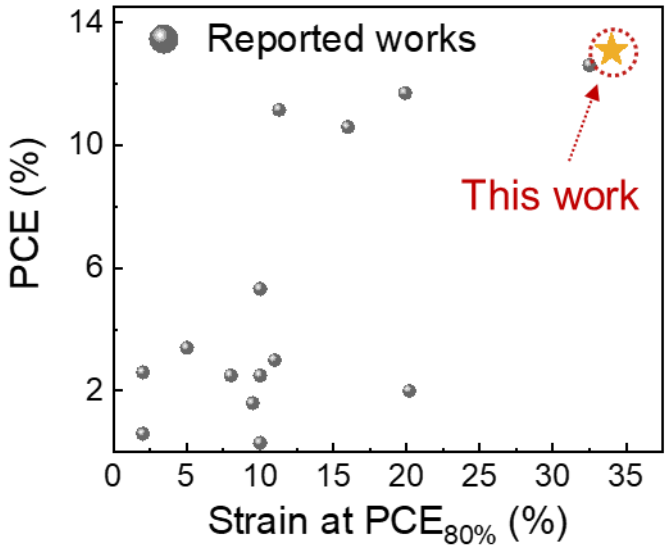


**Fig. S12.** PCE versus strain plots for IS-OSCs from the reported studies and this study.

**Table S11.** Device structures, mechanical and photovoltaic performances of reported IS-OSCs. The $PCE_{80\%}$ values were estimated by interpolation of the data reported in the papers.

| Year | Device structure | Active Layer | PCE [%] | Strain at $PCE_{80\%}$ [%] | Ref. |
|---|---|---|---|---|---|
| **2012** | UV/$O_3$-treated PDMS/PEDOT:PSS/Active Layer/EGaIn | P3HT:PCBM | ~1 | - | [1] |
| **2013** | PDMS/PEDOT:PSS/ Active Layer/EGaIn | P3HT:PCBM | 0.59 | - | [2] |
| | | P3DDT:PCBM | 0.29 | - | |
| **2016** | PU/PEDOT:PSS/PEI/Active Layer/PEDOT:PSS/PU | P3HpT:PCBM | 1.25 | - | [3] |
| **2017** | PUA-AgNW/ SWNT/PEDOT:PSS/Active Layer/PEIE/SWNT/ AgNW-PUA | PTB7-Th: $PC_{71}BM$ | 2.90 | - | [4] |
| **2017** | 3M tape/PEI/Ag/PH1000/ Active Layer/EGaIn | PTB7-Th: PCBM | 5.32 | 8.1 | [5] |
| | | PTB7-Th:N2200 | 2.02 | 20.2 | |
| **2018** | 3M tape/ PEDOT:PSS/ Active Layer/ PFN-NBR/EGaIn | PTB7-Th:N2200 | 2.02 | 20.2 | [6] |
| | | PTB7-Th: ITIC | 1.66 | 10.4 | |
| | | PTB7-Th: P(NDI2HD-T) | 3.00 | 15.7 | |
| **2019** | Ag mesh/PEDOT:PSS/ Active Layer/ PEIE/Ag/Parylene | PTzNTz: $PC_{71}BM$ | 9.70 | 7.7 | [7] |
| **2021** | PDMS/PH1000/ Active Layer/EGaIn | PBDB-T: PCE10:N2200 (1.2:0.8:1) | 6.33 | 11.2 | [8] |
| **2021** | TPU/PH1000/ AI4083/Active Layer/ PNDIT-F3N-Br/EGaIn | PM6:Y7 | 11.2 | 12.4 | [9] |
| | | PM6:PCBM | 5.7 | 5.1 | |
| | | PCE12:N2200 | 5.0 | 42.3 | |
| **2021** | TPU/AgNW/PEDOT:PSS/ Active Layer/EGaIn | PTB7-Th: IEICO-4F | 10.1 | 12.0 | [10] |
| **2022** | TPU/PH1000/ AI4083/Active Layer/ PNDIT-F3N-Br/EGaIn | PM6:Y7:N2200 (1:0.8:0.2) | 11.71 | 19.9 | [11] |
| **2022** | TPU/PH1000/ AI4083/Active Layer/ PNDIT-F3N-Br/EGaIn | PhAm5:Y7 | 12.7 | 31.6 | [12] |
| **2022** | MID-based TPU-PEDOT:PSS/ AI4083/Active Layer/ PNDIT-F3N-Br/EGaIn | PM6:Y6-BO:N2200 | **13.1** | **34.0** | **This Work** |

## References


1. D. J. Lipomi, J. A. Lee, M. Vosgueritchian, B. C. K. Tee, J. A. Bolander and Z. A. Bao, *Chem. Mater.*, 2012, **24**, 373-382.
2. S. Savagatrup, A. S. Makaram, D. J. Burke and D. J. Lipomi, *Adv. Funct. Mater.,* 2014, **24**, 1169-1181.
3. E. J. Sawyer, A. V. Zaretski, A. D. Printz, N. V. de los Santos, A. Bautista-Gutierrez and D. J. Lipomi, *Ext. Mech.Lett.*, 2016, **8**, 78-87.
4. L. Li, J. J. Liang, H. E. Gao, Y. Li, X. F. Niu, X. D. Zhu, Y. Xiong and Q. B. Pei, *ACS Appl. Mater. Interfaces*, 2017, **9**, 40523-40532.
5. Y. Y. Yu, C. H. Chen, C. C. Chueh, C. Y. Chiang, J. H. Hsieh, C. P. Chen and W. C. Chen, *ACS Appl. Mater. Interfaces*, 2017, **9**, 27853-27862.
6. Y. T. Hsieh, J. Y. Chen, S. Fukuta, P. C. Lin, T. Higashihara, C. C. Chueh and W. C. Chen, *ACS Appl. Mater. Interfaces*, 2018, **10**, 21712-21720.
7. Z. Jiang, K. Fukuda, W. C. Huang, S. Park, R. Nur, M. O. G. Nayeem, K. Yu, D. Inoue, M. Saito, H. Kimura, T. Yokota, S. Umezu, D. Hashizume, I. Osaka, K. Takimiya and T. Someya, *Adv. Funct. Mater.*, 2019, **29**, 1808378.
8. Q. L. Zhu, J. W. Xue, L. Zhang, J. L. Wen, B. J. Lin, H. B. Naveed, Z. Z. Bi, J. M. Xin, H. Zhao, C. Zhao, K. Zhou, S. Z. Liu and W. Ma, *Small*, 2021, **17**, 2007011.
9. J. Noh, G. U. Kim, S. Han, S. J. Oh, Y. Jeon, D. Jeong, S. W. Kim, T. S. Kim, B. J. Kim and J. Y. Lee, *ACS Energy Lett.*, 2021, **6**, 2512-2518.
10. Z. Y. Wang, M. C. Xu, Z. L. Li, Y. R. Gao, L. Yang, D. Zhang and M. Shao, *Adv. Funct. Mater.*, 2021, **31**, 2103534.
11. J.-W. Lee, G. U. Kim, D. J. Kim, Y. Jeon, S. Li, T. S. Kim, J. Y. Lee and B. J. Kim, *Adv. Energy Mater.*, 2022, **12**, 2200887.
12. J.-W. Lee, S. Seo, S. W. Lee, G. U. Kim, S. Han, T. N. Phan, S. Lee, S. Li, T. S. Kim, J. Y. Lee and B. J. Kim, *Adv. Mater.*, 2022, 2207544.